

Pressure filtration of colloidal SiC particles

Yoshihiro Hirata^{a,*}, Yosuke Tanaka^a, Seiya Nakagawa^b and Naoki Matsunaga^b

^aDepartment of Advanced Nanostructured Materials Science and Technology, Kagoshima University, 1-21-40 Korimoto, Kagoshima 890-0065, Japan

^bDepartment of Applied Chemistry and Chemical Engineering, Kagoshima University, 1-21-40 Korimoto, Kagoshima 890-0065, Japan

The consolidation behavior of colloidal SiC particles (30 or 800 nm diameter) with and without polyacrylic ammonium (dispersant, PAA) at pH 7 was examined using a developed pressure filtration apparatus in the pressure range from 100 kPa to 19 MPa at a constant crosshead speed or at a constant compressive pressure of a piston. In the electrostatically-stabilized colloidal suspensions (5 vol%-30 nm SiC (powder A), 30 vol%-800 nm SiC (powder B)) without PAA, a phase transition from a well-dispersed suspension to a flocculated suspension occurred when the applied pressure exceeded a critical pressure ($\Delta P_{ic} = 0.2\text{--}0.4$ MPa). The addition of PAA suppressed the phase transition. The height of the compressive piston as a function of filtration time at a constant applied pressure was simulated by an established filtration theory for a well-dispersed suspension and a newly-developed filtration theory for a flocculated suspension. The experimental results for both the suspensions of powders A and B with and without PAA were simulated well by the new model for flocculated suspension. The packing density of consolidated powders A and B in the filtration apparatus depended on the applied pressure, but the density after calcination was independent of the compressive pressure.

Key words: Pressure filtration, Phase transition, Dispersed particles, Flocculated particles.

Introduction

The technology of forming ceramic powder is divided into dry and wet processing methods. Uniaxial pressing and isostatic pressing are typical convenient dry forming methods. More uniform microstructures of green compacts are seen by wet forming methods such as filtration, pressure filtration [1-3], electrophoretic deposition [4-6] or doctor blading [7-9]. Pressure filtration can reduce the consolidation time of a colloidal suspension as compared with the filtration method using a gypsum mold because of a higher compressive pressure. The capillary tube suction pressure of a gypsum mold is 50-100 kPa, but the applied pressure of pressure filtration can be as high as 80 MPa when stainless steel equipment is used [10].

In previous papers [11-16], we analyzed the consolidation behavior of aqueous suspensions of hydroxyapatite, silicon carbide, 8 mol% yttria-stabilized zirconia, and alpha alumina powders in the size range from 20 to 800 nm using a newly-developed pressure filtration apparatus at a constant crosshead speed of a compressive piston or at a constant compressive pressure. From a comparison between the applied pressure (ΔP_i) and the volume of dehydrated filtrate (V_f), it was found that a phase transition from a dispersed state to a flocculated state occurs at a

critical applied pressure (ΔP_{ic}) [17]. Based on the colloidal phase transition, a new filtration theory was developed to explain the $\Delta P_i - h_i$ (height of piston) relation for a flocculated suspension. Good agreement was shown between the theory developed and experimental results of electrostatically-stabilized suspensions [14, 17]. In this paper, the effect of polyelectrolyte dispersant (polyacrylic ammonium, PAA) on the consolidation behavior of 30 and 800 nm SiC is studied at a constant compressive pressure (100 kPa-10 MPa) or at a constant crosshead speed of the piston. The measured h_i -filtration time relation is analyzed by both the established and newly-developed filtration theories.

Experimental procedure

Table 1 shows the characteristics of the SiC suspensions. A high purity α -SiC powder (powder A) supplied by Yakushima Electric Industry Co. Ltd., Kagoshima, Japan, was used in this experiment. A plasma CVD-processed β -SiC powder (powder B) supplied by Sumitomo Osaka Cement Co. Ltd., Tokyo, Japan, was also used. As-received powder A was dispersed at 30 vol% in an aqueous solution at pH 3.0 (named A3-30) and pH 7.0 (named A7-30). As-received powder B was dispersed at 5 vol% in an aqueous solution at pH 3.0 (named B3-5) and pH 7.0 (named B7-5). On the other hand, polyacrylic ammonium (PAA, $(\text{CH}_2\text{-CHCOONH}_4)_n$, molecular weight 10,000) of 0.36 mass% (0.27 mg/m²-SiC A) and 3.8 mass%

*Corresponding author:
Tel : +82-99-285-8325
Fax: +82-99-257-4742
E-mail: hirata@apc.kagoshima-u.ac.jp

Table 1. Characteristics of SiC suspensions

Suspension	Starting powder	Composition (mass %)	Median size (nm)	Specific surface area (m ² /g)	Solid content of suspension (vol %)	pH	PAA addition (mass %)
A3-30	α-SiC (powder A)	SiC 98.90,	800	13.4	30	7	0
A7-30		SiO ₂ 0.66,					
A7-30P		Al 0.004, Fe 0.013, Free C 0.37					
B3-5	β-SiC (powder B)	SiC 95.26,	30	50.9	5	7	0
B7-5		SiO ₂ 0.97,					
B7-5P		C 3.77					

PAA: Polacrylic ammonium (CH₂-CHCOONH₄)_n, molecular weight 10,000

(0.75 mg/m²-SiC B) was added to A7-30 (named A7-30P) and B7-5 (named B7-5P). The saturated amount of PAA adsorbed on the SiC surface at pH 7 was measured to be 0.29 mg/m² in our previous papers [18, 19]. That is, the prepared SiC suspensions contained the saturated amount of PAA or excess free PAA. The zeta potential of powders A and B with and without PAA was measured at a constant ionic strength of 0.01 M-NH₄NO₃ (Rank Mark II, Rank Brothers Ltd., Cambridge, UK) [18, 20]. The rheological behavior of the suspensions of powders A and B with and without PAA was measured by a cone and plate type viscometer (DV-II+Pro, Brookfield Eng. Lab., Massachusetts, USA). The prepared suspensions (A7-30, A7-30P, B7-5 and B7-5P) were consolidated through a plastic filter with a 20 μm pore diameter and three sheets of a membrane filter with a 0.1 μm pore diameter, which were attached to the bottom of the piston (polymeric resin) moving at a constant compressive pressure (0.1–10 MPa). When the suspension in a closed cylinder was compressed by the piston, the filtrate flowed into and through the pore channels formed in the upper piston. The applied load and the height of the piston were continuously recorded (Tensilon RTC, A & D Co. Ltd., Tokyo, Japan). The consolidated SiC compact was taken out of the cylinder and dried at 100 °C in air for 24 h. The dried compact was heated at 1000 °C in Ar atmosphere for 1 h to give an enough strength for the measurement of bulk density by the Archimedes method using kerosene.

Results and Discussion

Filtration models

A filtration process for the model structure shown in Fig. 1(a) is analyzed by Aksay and Schilling [21]. The total pressure drop ($P_t - P_0 = \Delta P_t$) across the mold ($P_0 - P_i = \Delta P_m$) and consolidated cake ($P_i - P_t = \Delta P_c$) is expressed by Eq.(1):

$$\Delta P_t t = -(\Delta P_c + \Delta P_m) t = \frac{1}{2} h_c^2 \eta n (\alpha_c + n \frac{\alpha_m}{\epsilon_m}) \quad (1)$$

where h_c is the height of consolidated layer, η the

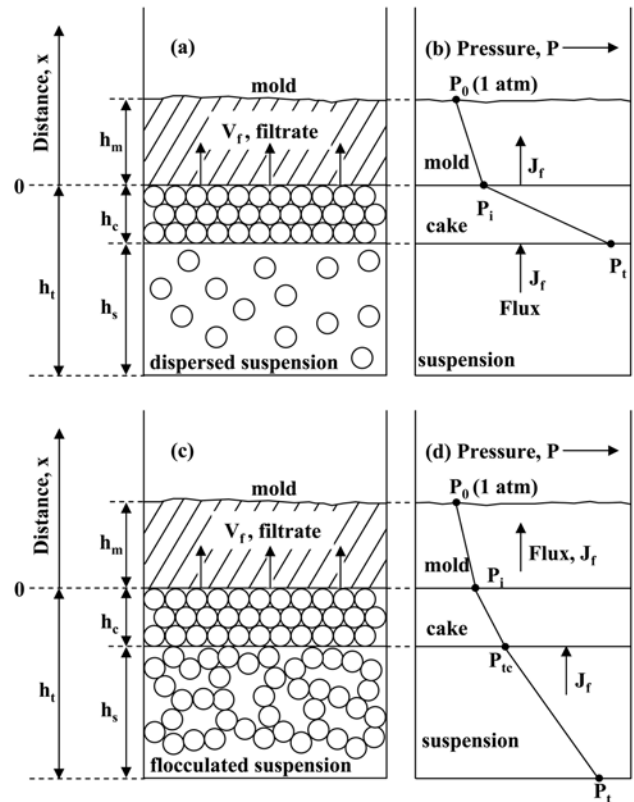


Fig. 1. Cross-sectional views of the filtration models (a, c) and hydraulic pressure profiles across the consolidated layer and the mold (b, d) for well-dispersed suspensions (a, b) and flocculated suspensions (c, d).

viscosity of the filtrate, n the system parameter ($\equiv (1 - C_0 - \epsilon_c)/C_0$, C_0 : the initial volume fraction of colloidal particles dispersed, ϵ_c : the volume fraction of voids in the consolidated layer), α_c the specific resistance of the porous consolidated layer, α_m the specific resistance of the porous medium, and ϵ_m the volume fraction of voids in the mold. When only the solution was compressed at a crosshead speed $v = 0.5$ mm/minute, ΔP_m was 5 ± 5 kPa. This value of ΔP_m was very small as compared with the experimental pressure range $\Delta P_t = 0.1$ –10 MPa and ΔP_m

can be neglected to ΔP_c . That is, Eq.(1) is approximated to Eq.(2):

$$\Delta P_t t \approx \frac{1}{2} h_c^2 \eta n \alpha_c \quad (2)$$

On the other hand, h_c is equal to $-V_f/nA$ and V_f/A is equal to $(H_0 - h_t)$, where V_f is the volume of filtrate, A the cross sectional area of the filtration apparatus, H_0 the initial height of the colloidal suspension and h_t (height of compressive piston) is equal to $(h_c + h_s)$ in Fig. 1(a). The above relations are substituted for Eq.(2) to obtain the measurable relation of Eq.(3):

$$\Delta P_t t = \frac{\eta \alpha_c}{2n} (H_0 - h_t)^2 \quad (3)$$

On the other hand, it was clarified in our previous paper that a phase transition from a dispersed suspension to a flocculated suspension occurs at a critical applied pressure (ΔP_{tc}) for nanoparticles of 20-800 nm size [17]. The ΔP_c depends on the zeta potential, the concentration and the size of colloidal particles. An increase of the zeta potential, a decrease of the particle concentration and an increase of particle size shift ΔP_{tc} to a high pressure [17]. Fig. 1(c, d) also shows the model structure and hydraulic pressure profile across the mold after the phase transition. In this model, the flux of filtrate is given by Eq.(4):

$$J_f = \frac{1}{A} \left(\frac{dV_f}{dt} \right) = -\frac{dh_t}{dt} = \frac{1}{\eta \alpha_s} \left(\frac{dP}{dh_s} \right) \quad (4)$$

where α_s is the specific resistance of the filtrate through the spaces among flocculated particles. The conditions of $P_{tc} = P_i$ and h_{sc} (height of flocculated suspension at ΔP_{tc}) = H_0 correspond to an early particle compaction without a consolidated layer of dispersed particles. The pressure drop for this initially flocculated suspension is described by Eq.(5):

$$\frac{dP}{dh_s} = -\eta \alpha_s \left(\frac{dh_s}{dt} \right) = \frac{P_i - P_t}{h_s} \quad (5)$$

Under a constant pressure difference of $P_i - P_t$ (= $-\Delta P_s$), Eq.(5) can be integrated as follows:

$$-\int_0^t \Delta P_s dt = -\Delta P_s t = \int_{H_0}^{h_s} \eta \alpha_s h_s dh_s \quad (6)$$

When α_s is determined as a function of h_s , we can integrate the right term of Eq.(6). The fractions of particles (C) and solution ($1 - C$) of the flocculated suspension of height h_s are given by Eqs.(7) and (8), respectively:

$$C = C_0 \left(\frac{H_0}{h_s} \right) \quad (7)$$

$$1 - C = 1 - C_0 \left(\frac{H_0}{h_s} \right) \quad (8)$$

According to the Kozeny-Carman model [21], the specific

porous medium resistance α is expressed by Eq.(9):

$$\alpha = \frac{BS^2(1-\varepsilon)^2}{\varepsilon^3} \quad (9)$$

where B is the ratio of the shape factor to the tortuosity constant, S the ratio of the total solids surface area to the apparent volume of the consolidated system and ε the porosity of the particle layer. In the flocculated suspension, $(1 - C)$ is equivalent to ε and C corresponds to $(1 - \varepsilon)$ in Eq.(9). This simulation enables a correlation of α_s with h_s as follows:

$$\alpha_s = BS^2 (H_0 C_0)^2 \frac{h_s}{(h_s - H_0 C_0)^3} \quad (10)$$

That is, the pressure drop $-\Delta P_s$ (= $P_t - P_i$) for an initially flocculated suspension is calculated by Eq.(11):

$$-\Delta P_s t = \eta BS^2 (H_0 C_0)^2 \int_{H_0}^{h_s} \frac{h_s^2}{(h_s - H_0 C_0)^3} dh_s \quad (11)$$

where BS^2 is treated as a constant value. The integration of the right term, named as $R(h_s)$, is given by Eq.(12):

$$R(h_s) = \frac{1}{2} \left[\frac{h_s^2}{(h_s - H_0 C_0)^2} - \frac{H_0^2}{(H_0 - H_0 C_0)^2} \right] + \left[\frac{h_s}{(h_s - H_0 C_0)} - \frac{H_0}{(H_0 - H_0 C_0)} \right] + \ln \left(\frac{H_0 - H_0 C_0}{h_s - H_0 C_0} \right) \quad (12)$$

Since $-\Delta P_s$ becomes greatly larger than $-\Delta P_m$ with decreasing h_s , $-\Delta P_s$ gives a good approximation of ΔP_t (= $P_t - P_0$). Equations (3) and (11) were compared with the experimental results.

Zeta potential and rheology of SiC suspensions

Fig. 2 shows the zeta potential of powders A and B with and without PAA as a function of suspension pH.

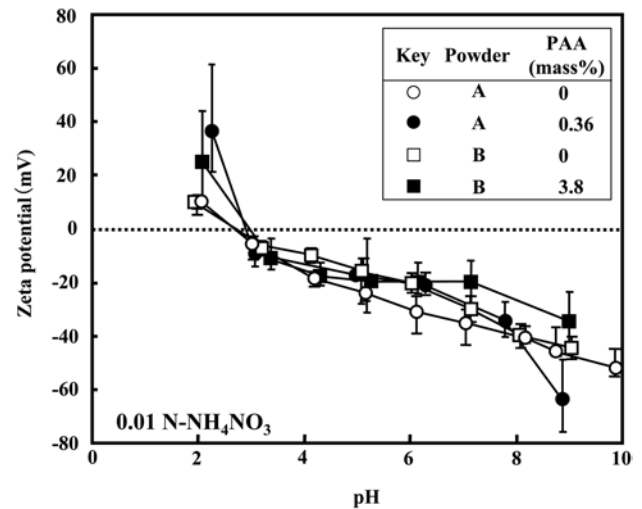


Fig. 2. Zeta potential of the powders A and B with and without PAA as a function of suspension pH.

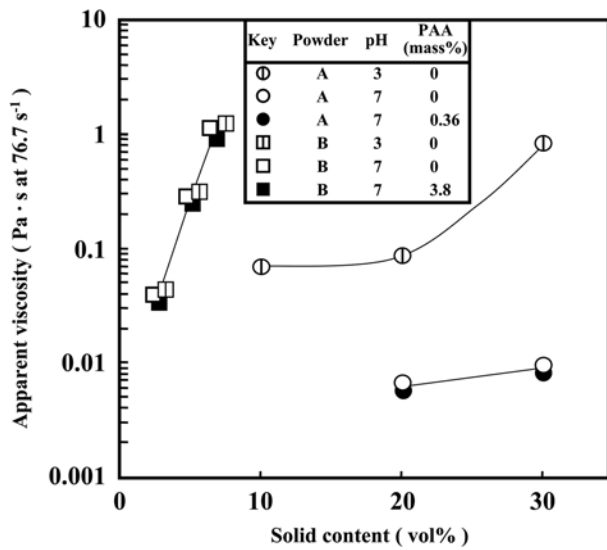


Fig. 3. Apparent viscosity of aqueous suspensions of 30 and 800 nm SiC particles with and without PAA at pH 3 and 7.

As-received powders A and B were charged positively at 11 mV at pH 1.9 and negatively above pH 3.0. Both the isoelectric points were pH 2.8. When PAA was added to the suspensions, the surface potential of powders A and B increased to 28-40 mV at pH 2.0-2.1. However, no significant change of the isoelectric point was measured with the addition of PAA. In the wide pH range, the SiC particles with and without PAA were charged negatively. Dissociation of PAA starts at about pH 3 and reaches 100% at about pH 9 [22]. However, this effect of PAA on the surface potential of SiC was small as seen in Fig. 2.

Fig. 3 shows the apparent viscosity at a shear rate of 76.7 s^{-1} for the powders A and B with and without PAA at pH 3 and 7 as a function of solid content [11, 23]. The viscosity of powder A suspension without PAA decreased with an increase of pH or with a decrease of solid content. This result is related to the increased dispersibility of powder A at pH 7 due to the high repulsive energy or increased distance between two particles (Fig. 2). The addition of PAA gave no significant influence on the low viscosity of the suspension at pH 7. On the other hand, the viscosity of powder B suspension, which was relatively high at 3-7 vol% solid, was almost independent of pH, indicating a small influence of surface potential of 30 nm particles on the viscosity. That is, powder B has a strong tendency to make a flocculated particle network in the aqueous suspension at pH 3 and 7 [11, 23]. The addition of PAA dissociated at pH 7 provided little effect on the dispersion of the particle network of powder B.

Pressure filtration of SiC suspensions at a constant crosshead speed of piston

Fig. 4 shows the typical relationship between applied pressure (ΔP_t) and normalized volume of the dehydrated solution (V_f/V_0 , V_0 : volume of initial suspension) for (a) A7-30 and (b) A7-30P suspensions at a constant

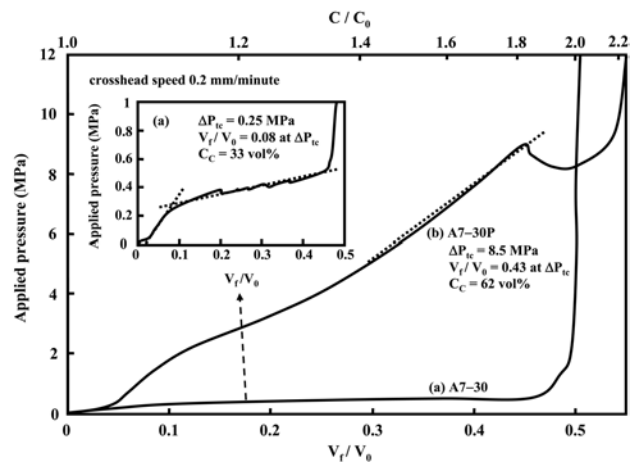


Fig. 4. Typical relationship between applied pressure (ΔP_t) and normalized volume of dehydrated solution (V_f/V_0 , V_0 : volume of initial suspension) for (a) A7-30 and (b) A7-30P suspensions at a constant crosshead speed of the compressive piston ($v = 0.2 \text{ mm/minute}$).

crosshead speed of piston ($v = 0.2 \text{ mm/minute}$). According to the model structure in Fig. 1(a), ΔP_c at a constant crosshead speed of piston is expressed by Eq.(13):

$$\Delta P_c = \left(\frac{\eta \alpha_c v}{nA} \right) V_f = \left(\frac{\eta \alpha_c v}{n} \right) (H_0 - h_t) \quad (13)$$

This equation indicates a linear relation of ΔP_c and V_f .

As seen in Fig. 4(a), the applied pressure of the A7-30 suspension increased linearly with an increase of V_f as predicted by Eq.(13). However, the deviation of ΔP_t from the theory started at 0.25 MPa of applied pressure, indicating the phase transition from the dispersed to the flocculated suspension. The $\Delta P_t - V_f$ relation after the phase transition is simulated well by the filtration theory derived for a flocculated suspension. The detailed derivation of the $\Delta P_t - V_f$ relation is presented in our previous paper [17]. On the other hand, the A7-30P suspension showed a linear relation over a wide pressure range. The ΔP_{ic} was estimated to be 8.5 MPa. Although no significant difference was measured in the viscosity for the suspensions with and without PAA (Fig. 3), the consolidation behavior was greatly affected by the addition of PAA. At 8.5 MPa of ΔP_t for the A7-30P suspension, the solid content of the suspension reached 62 vol% and was close to the density of random close packing (63.7%) [24]. The increased pressure in the final stage may be related to the elastic compression of the adsorbed PAA layers [17]. The adsorption of PAA on powder A suppressed the phase transition and the dispersed particles were densely consolidated.

Fig. 5 shows the relationship between the applied pressure (ΔP_t) and the normalized volume of the dehydrated solution for (a) B7-5 and (b) B7-5P suspension. The consolidation behavior of Fig. 5(a) was similar to that of Fig. 4(a) and the ΔP_{ic} was estimated to be 0.32 MPa. This result indicates that (1) ΔP_{ic} is a similar value for 30 and 800 nm SiC

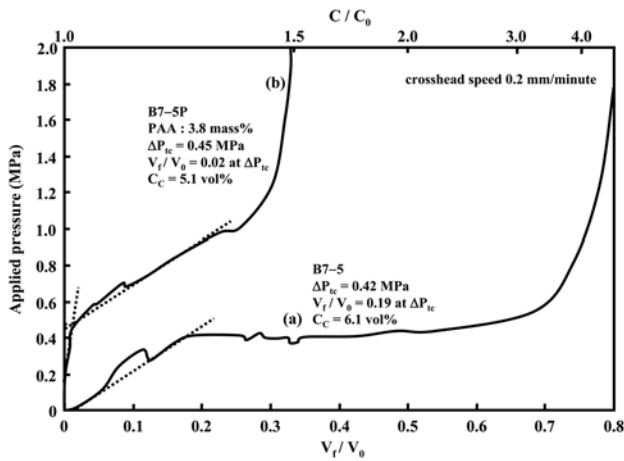


Fig. 5. Typical relationship between applied pressure (ΔP_t) and normalized volume of the dehydrated solution for (a) B7-5 and (b) B7-5P suspensions at a constant crosshead speed of the compressive piston ($v = 0.2$ mm/minute).

particles and (2) the solid content (C_c) at ΔP_{tc} is significantly lower for 30 nm particles than for 800 nm particles. When the distance between dispersed particles becomes smaller, the phase transition occurs easily at a low concentration of particles. On the other hand, the PAA-added suspension of powder B showed a rapid increase of ΔP_t at the initial stage of the filtration, followed by a linear increase of ΔP_t with increasing V_f . This consolidation behavior suggests (1) a dense particle layer is formed at

the initial stage of filtration and (2) a similar dense second layer is formed in the subsequent stage of filtration. This result is also related to the adsorption of PAA on powder B. However, the ΔP_t value increased greatly at a small value of V_f . This result reflects the difficulty of elimination of the solution through PAA layers compressed in the small spaces among 30 nm particles. On the other hand, the solution in the flocculated particles (Fig. 5(a)) is easily eliminated at a low pressure. As seen in Figs. 4 and 5, the adsorption of PAA on SiC particles suppresses the phase transition and increases the pressure during the filtration.

Filtration kinetics of SiC suspension at a constant pressure

Fig. 6 shows the relation between the height of the piston (h_t) and the filtration time of SiC suspensions at $\Delta P_t = 0.1$ MPa (a, b) and 10 MPa (c, d) for A7-30 (a, c) and A7-30P suspensions (b, d). The data in Fig. 4 suggest that the SiC suspensions with and without PAA contained dispersed particles at $\Delta P_t = 0.1$ MPa. The experimental results were analyzed by Eqs.(3) and (11). The measured h_t in Fig. 6(a, b) decreased nonlinearly as a function of filtration time and Eq.(3) for the filtration of dispersed particles showed good simulation. Equation (11) for the filtration of flocculated particles also simulated well the measured h_t values. The above good simulation provides the interpretation that (1) Eq.(11) gives a good approximation of Eq.(3) and (2) in an actual filtration

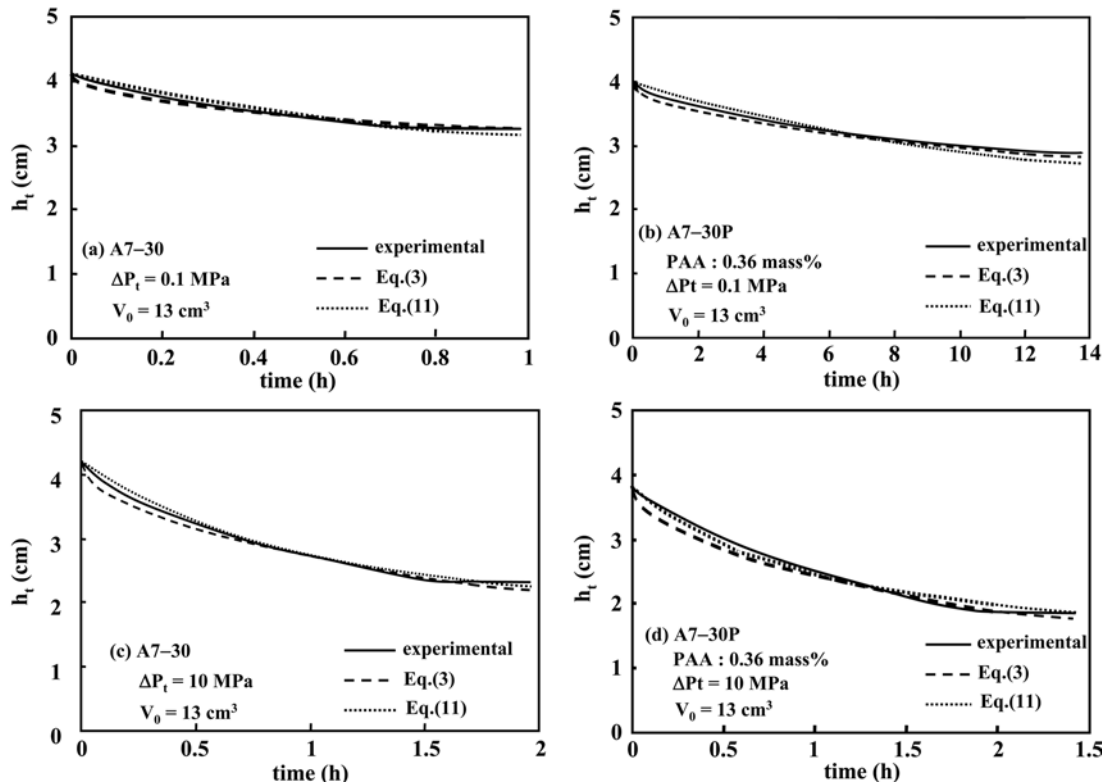


Fig. 6. Relation between the height of the piston (h_t) and the filtration time of SiC suspensions at $\Delta P_t = 0.1$ MPa (a, b) and 10 MPa (c, d) for A7-30 (a, c) and A7-30P suspensions (b, d) at pH 7.

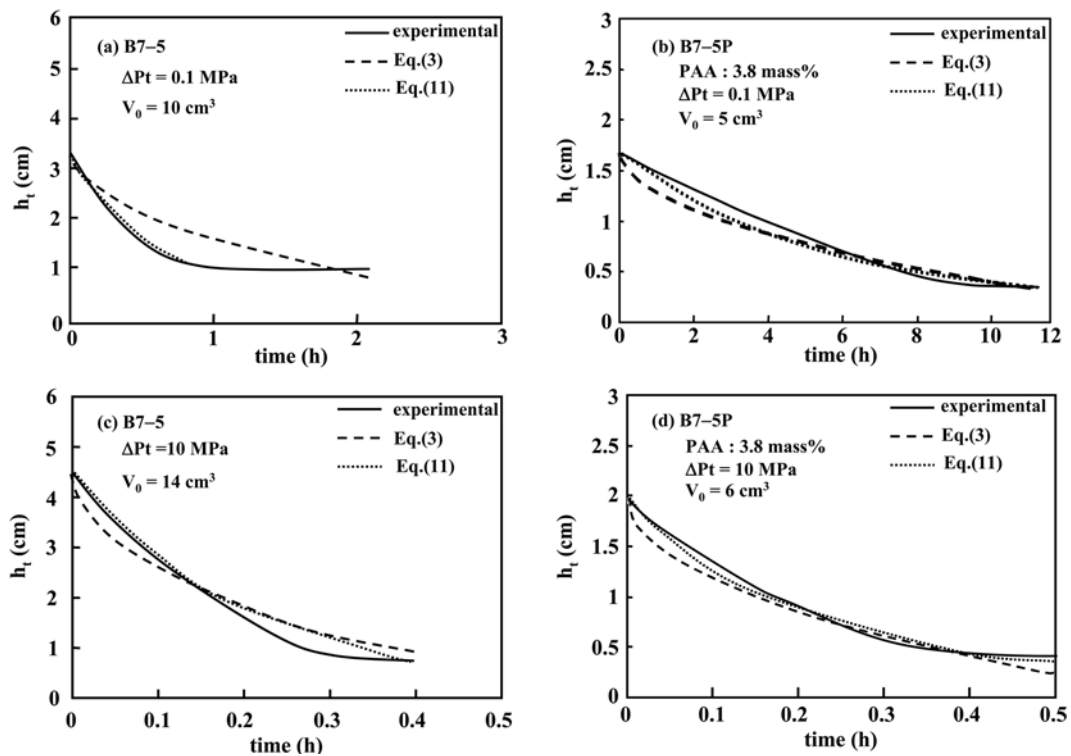


Fig. 7. Relation between the height of the piston (h_t) and the filtration time of SiC suspensions at $\Delta P_t = 0.1$ MPa (a, b) and 10 MPa (c, d) for B7-5 (a, c) and B7-5P suspensions (b, d) at pH 7.

of the SiC A powder at a low applied pressure, the mixed states of dispersed and flocculated particles may be consolidated. At a high pressure of 10 MPa which was higher than the estimated ΔP_{tc} for A7-30 and A7-30P suspensions (Fig. 4), a good agreement was recognized between the results (c and d) and Eq.(11). As compared with Eq.(11), a larger deviation was observed between the results and Eq.(3), indicating that flocculated particles were filtrated at $\Delta P_t = 10$ MPa.

Fig. 7 shows the relation between h_t and the filtration time at $\Delta P_t = 0.1$ MPa (a, b) and 10 MPa (c, d) for B7-5 (a, c) and B7-5P suspensions (b, d). According to the experiment in Fig. 5, the SiC particles are interpreted to remain in a dispersed state at $\Delta P_t = 0.1$ MPa. However, the measured h_t values at $\Delta P_t = 0.1$ MPa were well simulated by Eq.(11) rather than Eq.(3). The above comparison leads to the interpretation that the SiC B particles have a strong tendency to make particle clusters with an increase in time even at the low applied pressure of 0.1 MPa. The result in Fig. 7(a) is supported by the high viscosity measured in Fig. 3. Addition of PAA gave a small influence on the viscosity. This result is reflected in Fig. 7(b) especially during the period within 1 h. A care should be placed on the filtration time to compare the results of Figs. 7(a) and (b). A long filtration time at a low pressure in Fig. 7(b) indicates the difficulty of eliminating the solution through the compressed flocculated particle clusters with PAA. This observation agreed with the interpretation for the result in Fig. 5(b). At a higher pressure of $\Delta P_t = 10$ MPa, both the results in Fig. 7(c) and (d) were well simulated

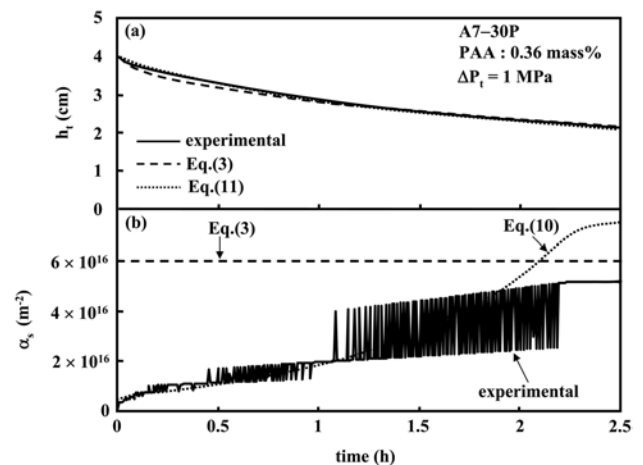


Fig. 8. Relation between the filtration time and (a) the height of the piston or (b) specific resistance of filtration for the A7-30P suspension.

by Eq.(11) and the filtration time was shortened. The flocculated particle clusters were compressed shortly at 10 MPa of ΔP_t . A more detailed discussion is reported in the next section using the specific filtration resistance of filtration.

Specific resistance of filtration and packing density of consolidated cake

Fig. 8 shows the relationship between the filtration time and h_t (a) or the specific resistance of filtration (b) for the A7-30P suspension at 1 MPa. The observed specific

resistance value (α_s) was determined by Eq.(14) based on Eqs.(4) and (5) using the measured h_t in Fig. 8(a):

$$\alpha_s(\text{observed}) = \frac{\left(\frac{\Delta P_t}{h_t}\right)}{\eta\left(-\frac{\Delta h_t}{\Delta t}\right)} \quad (14)$$

The Δt was set to 1 minute to measure the difference of h_t . On the other hand, Eqs.(3) and (10) were used to simulate α_s for the dispersed and flocculated suspensions, respectively. The n value in Eq.(3) was calculated using the final packing density after the filtration. As seen in Fig. 8(b), the observed α_s increased gradually with an increase in the filtration time. The sharp deviation in α_s is due to the change of ΔP_t . The change of ΔP_t was 2.4-10% in the pressure range of 0.1-1.0 MPa and less than 1% at 3-10 MPa. The α_s value in Eq.(3) was treated as a constant value to simulate the whole filtration process. This simulation caused a relatively large difference of α_s values between the experiment and calculation. On the other hand, Eq.(10) can represent the time dependence of α_s using the measured h_t value. This simulation provided a good agreement of α_s values between the experiment and calculation. A similar comparison was also observed for the α_s values of the B7-5 and B7-5P suspensions. As seen in Fig. 8, the accurate filtration process can be understood by α_s value rather than h_t value. The result in Fig. 8(b) suggests that the structural model in Fig. 1(c) is effective to simulate the consolidation behavior of submicrometre-sized particles with PAA.

Fig. 9 shows the BS^2 value in Eq.(10) as a function of the applied pressure. The increased solid content in the flocculated suspension causes an increase of the specific surface area (S) at a given particle size. The whole BS^2 values show generally a tendency of an increase with an increase in the applied pressure. In the pressure range below 0.6 MPa, the consolidation behavior of 30 and 800 nm SiC particles is greatly influenced by the addition of

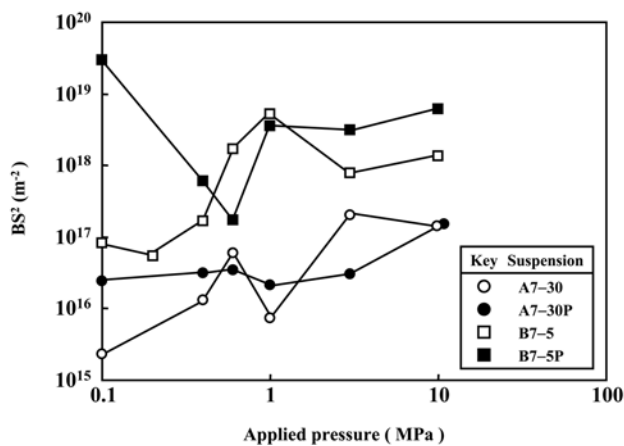


Fig. 9. BS^2 value of Eq. (10) in the text as a function of applied pressure.

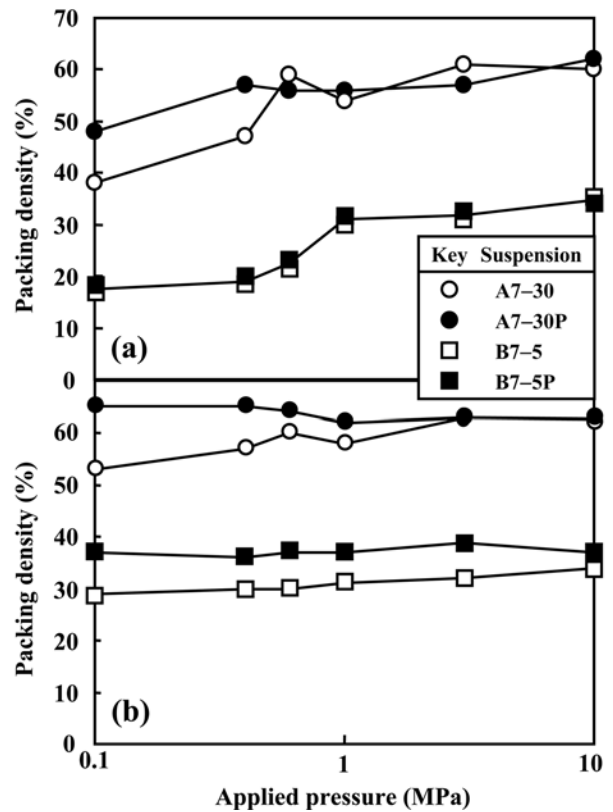


Fig. 10. Packing density of powders A and B without and with PAA after filtration (a) and the density after calcination at 1000 °C in an Ar atmosphere (b).

PAA. The difference in BS^2 values with PAA became small at a higher pressure. This result was already discussed previously. The BS^2 value was larger for 30 nm SiC than for 800 nm SiC. A decrease of particle size increases the S value, resulting in the increased α_s value. The BS^2 value in Fig. 9 is directly related to the magnitude of the α_s value.

Fig. 10(a) shows the packing density of A7-30, A7-30P, B7-5 and B7-5P suspensions after filtration. The data in Fig. 10(a) reflect well the BS^2 values in Fig. 9. The packing density of A7-30 and A7-30P suspensions increased gradually from 38% at $\Delta P_t = 0.1$ MPa to 62% at $\Delta P_t = 10$ MPa. In the low pressure range ($\Delta P_t < 0.4$ MPa), the addition of PAA enhanced the packing density. The adsorption of PAA on 800 nm SiC particles leads to the dense packing during the consolidation at a low pressure. Similarly, the packing density of B7-5 and B7-5P suspensions increased from 17% at $\Delta P_t = 0.1$ MPa to 35% at $\Delta P_t = 10$ MPa. Little difference in the packing density was measured with the addition of PAA. However, a large BS^2 value was measured for the B7-5P suspension at $\Delta P_t = 0.1$ MPa (Fig. 9). This discrepancy may be explained by the conformation of the adsorbed PAA. Fig. 10(b) shows the green density of SiC powders after the calcination at 1000 °C. After the calcinations, the low packing density for the compacts consolidated at a low pressure range (< 1 MPa) was increased. This result is related to the

shrinking of the wet compacts during the drying at room temperature. As seen in Fig. 10, the drying effect on the green density was high for the compacts with PAA. The change of conformation of PAA during the drying accelerates the shrinking of the powder compacts.

Conclusions

The adsorption of PAA on 30 and 800 nm SiC particles at pH 7 suppressed the phase transition from the dispersed to flocculated suspension during the filtration at a constant crosshead speed of a compressive piston. The phase transition pressure (ΔP_{tc}) had a similar value for 30 and 800 nm SiC particles without PAA but the solid content at ΔP_{tc} was significantly lower for 30 nm SiC particles than for 800 nm SiC particles. A high pressure was needed to eliminate the solution through the PAA layers compressed in the small spaces among SiC particles. However, the solution in the flocculated particle clusters without PAA was easily filtrated at a low applied pressure. The filtration theory developed at a constant applied pressure for a flocculated suspension gave a good approximation of the height of the compressive piston as a function of time for the suspensions of 30 and 800 nm particles with and without PAA. The specific resistance of filtration gradually increased with filtration time and was well simulated by the filtration theory developed. The packing density of the consolidated particles was closely related to the value of BS^2 in the theory, where B is the ratio of the shape factor to the tortuosity constant and S the ratio of the total solids surface area to the apparent volume of the consolidated system.

References

1. P.C. Kapur, S. Laha, S.P. Usher, R.G. deKretser and P.J. Scales, *J. Colloid and Inter. Sci.* 256[1] (2002) 216-222.
2. E. Vorobiev, *Chem. Eng. Sci.* 61[11] (2006) 3686-3697.
3. S. Raha, K.C. Khilar, P.C. Kapur and Pradip, *Int. J. Process.* 84[1-4] (2007) 348-360.
4. J. Will, M.K.M. Hruschka, L. Gubler and L.J. Gauckler, *J. Am. Ceram. Soc.*, 84[2] (2001) 328-332.
5. B.D. Hatton and Y. Sakka, *J. Am. Ceram. Soc.*, 84[3] (2001) 666-668.
6. Y.C. Wang, I.C. Leu and M.H. Hon, *J. Am. Ceram. Soc.*, 87[1] (2004) 84-89.
7. J.X. Zhang, D.L. Jiang, S.H. Tan, L.H. Gui and M.L. Ruan, *J. Am. Ceram. Soc.*, 84[11] (2001) 2537-2541.
8. S. Uchida, S. Sameshima and Y. Hirata, *J. Ceram. Soc. Japan*, 109[2] (2001) 100-105.
9. A.I. Kontos, A.G. Kontos, D.S. Tsoukleris, M.C. Bernard, N. Spyrellis and P. Falaras, *J. Mater. Process. Tech.*, 196[1-3] (2008) 243-248.
10. F.F. Lange and K. T. Miller, *Am. Ceram. Soc. Bull.*, 66 [10] (1987) 1498-1504.
11. Y. Hirata, M. Nakamura, M. Miyamoto, Y. Tanaka and X. H. Wang, *J. Am. Ceram. Soc.*, 89[6] (2006) 1883-1889.
12. K. Kishigawa and Y. Hirata, *J. Eur. Ceram. Soc.*, 26[1-2] (2006) 217-221.
13. K. Kishigawa and Y. Hirata, *J. Ceram. Soc. Japan*, 114[3] (2006) 259-264.
14. Y. Tanaka, Y. Hirata, N. Matsunaga, M. Nakamura, S. Sameshima and T. Yoshidome, *J. Ceram. Soc. Japan*, 115[11] (2007) 786-791.
15. Y. Hirata and Y. Tanaka, *Proceedings of 6th Pacific Rim Conference on Ceramic and Glass Technology (CDR)*, The American Ceramic Society (2006).
16. Y. Hirata, Y. Tanaka and Y. Sakamoto, *Advances in Science and Technology*, 45 (2006) 471-479.
17. Y. Hirata and Y. Tanaka, *J. Am. Ceram. Soc.*, 91[3] (2008) 819-824.
18. Y. Hirata, S. Tabata and J. Ideue, *J. Am. Ceram. Soc.*, 86[1] (2003) 5-11.
19. Y. Hirata, S. Tabata and J. Ideue, *Advances in Science and Technology*, 30 (2003) 545-554.
20. N. Hidaka and Y. Hirata, *J. Ceram. Soc. Japan*, 113 [7] (2005) 466-472.
21. I.A. Aksay and C.H. Schilling, *Advances in Ceramics*, Vol. 9, *Forming of Ceramics*, Edited by J.A. Mangels and G.L. Messing, The American Ceramic Society, Columbus, (1984) 85-93.
22. Y. Hirata, J. Kamikakimoto, A. Nishimoto and Y. Ishihara, *J. Ceram. Soc. Japan*, 100[1] (1992) 7-12.
23. Y. Hirata and Y. Tanaka, *Bull. Ceram. Soc. Japan*, 42[2] (2007) 87-92.
24. J.M. Ziman, "Models of Disorder", Cambridge University Press, Oxford, (1979) 78-87.